Green Synthesis of novel *Rhododendron arboreum* Based Zinc Nanocomposites for Enhanced Antimicrobial and Photocatalytic Degradation Activities

Sajid Ali *, Sidra - , Tanveer Asghar , Muhammad Ishtiaq Jan *, Muhammad Waqas , Tahir Ali , Riaz Ullah , Ahmed Bari

Posted Date: 11 April 2024

doi: 10.20944/preprints202404.0675.v2

Keywords: *Rhododendron arboreum*; Zinc nanoparticles; Antimicrobial activity; Photocatalyst; Methyl orange dye

 doi:10.20944/preprints202404.0675.v2

Article

Green Synthesis of Novel *Rhododendron arboreum* Based Zinc Nanocomposites for Enhanced Antimicrobial and Photocatalytic Degradation Activities

Sajid Ali [1,*], Sidra [1], Tanveer Asghar [1] Muhammad Ishtiaq Jan [2], Muhammad Waqas [3], Tahir Ali [4], Riaz Ullah [5] and Ahmed Bari [6]

[1] Department of Chemistry, Bacha Khan University, Charsadda 24420, Khyber Pakhtunkhwa, Pakistan
[2] Department of Chemistry, Kohat University of Science and Technology, Kohat 26000, Khyber Pakhtunkhwa, Pakistan
[3] Department of Environmental Sciences, Kohat University of Science and Technology, Kohat 26000, Khyber Pakhtunkhwa, Pakistan
[4] State Key Laboratory of Chemical Oncogenomics, Peking University Shenzhen Graduate School, Shenzhen, Guangdong, 518055, PR China
[5] Department of Pharmacognosy, College of Pharmacy, King Saud University, Riyadh 11451, Saudi Arabia
[6] Department of Pharmaceutical Chemistry, College of Pharmacy, King Saud University, Riyadh 11451, Saudi Arabia
* Correspondence: sajidali.faculty@bkuc.edu.pk; mishtiaqjan@kust.edu.pk

Abstract: Zinc nanoparticles (ZnNPs) open new opportunities for biomedical applications as a strategy against microbes and dye removal in an efficient way. The composite ZnNPs using *Rhododendron arboreum (R. arboreum)* stem bark were synthesized and characterized for UV-visible spectroscopy (UV-vis), Fourier transform infrared spectroscopy (FTIR), energy dispersive X-ray spectroscopy (EDX), scanning electron microscopy (SEM), and X-ray diffraction (XRD). The synthesized nanoparticles showed zones of inhibition of 23±0.09, 18±0.1 and 16±0.05 mm, against the *Klebsiella pneumoniae* (*K. pneumoniae)*, *Staphylococcus aureus (S. aureus)* and *Escherichia coli* (*E. coli* strains. The minimum inhibitory concentration (MIC) and minimum bactericidal concentration (MBC) values against *K. pneumoniae*, *S. aureus,* and *E. coli* were found to be 34±0.21 and 72.71±0.47, 47±0.11 and 94.86±0.84 and 94±0.18 and 185.43±0.16 µg/mL, respectively. The biosynthesized ZnNPs resulted in significant eradication of the outer and inner membranes of the bacterial cells. Likewise, the synthesized ZnNPs showed time-dependent photocatalytic degradation activity and revealed 65% methyl orange dye degradation with an irradiation period of 6 hours. The findings of this study suggest the suitability of the novel *R. arboreum* stem bark-based ZnNPs as an effective ameliorant against bactericidal activities and photocatalysts for the removal of hazardous water contaminants.

Keywords: *Rhododendron arboreum;* zinc nanoparticles; antimicrobial activity; photocatalyst; methyl orange dye

1. Introduction

In developing countries, the problem of sanitization especially for infections caused by water attained considerable attention during the last few decades[1]. The threats of waterborne infections may be microbial, chemical, and/or physical [2]. In the case of microbial infections, the alarming situation is when specific microbe(s) acquire strong resistance to antibiotics [3]. It has been well reported that several groups of antibiotics became less effective against many microbial strains. Likewise among chemicals, dyes are groups of toxins produced from a series of anthropogenic activities and are released into the water environment [1]. The majority of organic dyes utilized in several industries including those used in textile, paper, paints, and medicine are non-biodegradable [4]. In addition to the environmental problems, dyes are of significant concern because of their extremely hazardous nature causing various health-related problems including excessive perspiration, cognitive confusion, and methemoglobonemia [5]. It has been estimated that in the dying process, about 10% of the total dyes are consumed while all the remaining amount is

 doi:10.20944/preprints202404.0675.v2

discharged to the water resources without proper treatment and poses serious threats to the aquatic life by reducing the oxygen supply and the algal photosynthetic ability in water [6].

The researchers are now focused on the development of such strategies to protect human and environmental health effectively and economically [7]. Among the advanced research trends, nanotechnology is an emerging research area in the fields of biomedicine, engineering, and bioremediation [8]. The key features that account for the effectiveness of nanoparticles include small size, high surface area, morphologies, ultraviolet-protective, photocatalytic, and antimicrobial properties that make them a promising candidate in several fields including environment, medicine, and agriculture [9]. Likewise, among nanoparticles, metal-based nanoparticles have gained much attention due to their unique electrochemical, biological and optical properties along with biocompatibility and non-toxic effects [10]. Against microbes, nanoparticles target multiple biomolecules at once and hence prevent the development of microbial resistance [11]. It has been well understood that nanoparticles with antibacterial potentials can reduce the development of resistance by specific microbes [12]. Likewise, due to their unique characteristics including larger excitation binding energy and wide band gap metal nanoparticles are considered as an attractive photocatalyst for the degradation of dyes [13].

Nanoparticles can be synthesized through several methods such as microwave, sol-gel, hydrolysis, and co-precipitation methods [14]. However, green nanotechnology is more significant than other chemical and physical technologies due to their low cost and eco-friendly nature. Several researchers successfully investigated the biosynthesis of nanomaterials by using different types of biological sources including bacteria, fungi, and plant extracts[15]. However, it is important to note that the composite of nanoparticles with plants showed better results as compared to other biological systems. It is because the process of utilizing the plants for the green synthesis is economical in comparison to the process involved in using other agents like algae, and fungi [16]. In addition, the composite of nanoparticles with various plants and their parts acts differently as both reducing and stabilizing agents [17]. Many plant products have been successfully reported as capping agents for the stabilization of nanoparticles in the literature [18]. However, metal-based nanoparticles using *R. arboreum* stem bark have not received much attention in the literature. *R. arboreum* a member of the family Ericaceae is one of the most important medicinal plants. This plant is distributed throughout the world mostly centered to China, India, Malaysia, and Nepal [19]. In Pakistan, this plant occurs in the Hazara Division and Kashmir. Due to the presence of several bioactive compounds, the various parts of *R. arboreum* have several medicinal applications and are used to treat diarrhea, blood dysentery, and headache. The stem bark of the *R. arboreum* contains a variety of compounds which include 15-oxoursolic acid, ursolic acid, betulinic acid, lupeol, taraxerol, β-amyrine, 3-O-acetyl ursolic acid, 3β- acetoxyurs- 11-en-13β, 28-olide, 3-O-acetylbetulinic acid [20]. Based on the available information, the current investigation for the first time synthesized ZnNPs from the bark extract of *R. arboreum* with the aim to exploit the underlying bactericidal mechanisms against several pathogenic bacteria and its role towards environmental remediation for the photocatalytic degradation of methyl orange dye.

2. Results

2.1. UV-Visible Spectrophotometry and Fourier Transform Infrared Analysis

UV-visible spectrometry is a crucial approach since each metal nanoparticle displayed a different surface plasmon resonance value. The synthesized ZnNPs were therefore validated by UV-visible spectrometric and the results are illustrated in the Figure 1a. The spectrum of the surface plasmon resonance at 374 nm suggested the production of ZnNPs, as seen in the UV-visible spectrum. The biosynthesized ZnNPs revealed a distinctive spectrum characteristics that zinc exhibited neither in bulk metals nor in molecular form. Moreover, the FTIR spectra of nanoparticles prepared with *R. arboreum* were also carried out for the determination of various functional groups. The FTIR spectrum of green synthesized ZnNPs by extract of *R. arboreum* is shown in Figure 1b. The FTIR spectrum displayed various peaks at 2921, 1700, 1570, 1363, 798, 522, and 453 cm^{-1}. The peaks observed at 2921 and 1700 cm^{-1} correspond to O-H and C-H bond stretching. Similarly, the peaks at 1570, 1363 , and

 doi:10.20944/preprints202404.0675.v2

798cm^{-1} indicated the presence of a C=O bond and symmetric bending of CH_3, respectively. The intense peaks at 522 cm^{-1} were attributed to C-C and N-H vibration. The formation of ZnNPs were confirmed by the major peak at 453 cm^{-1}.

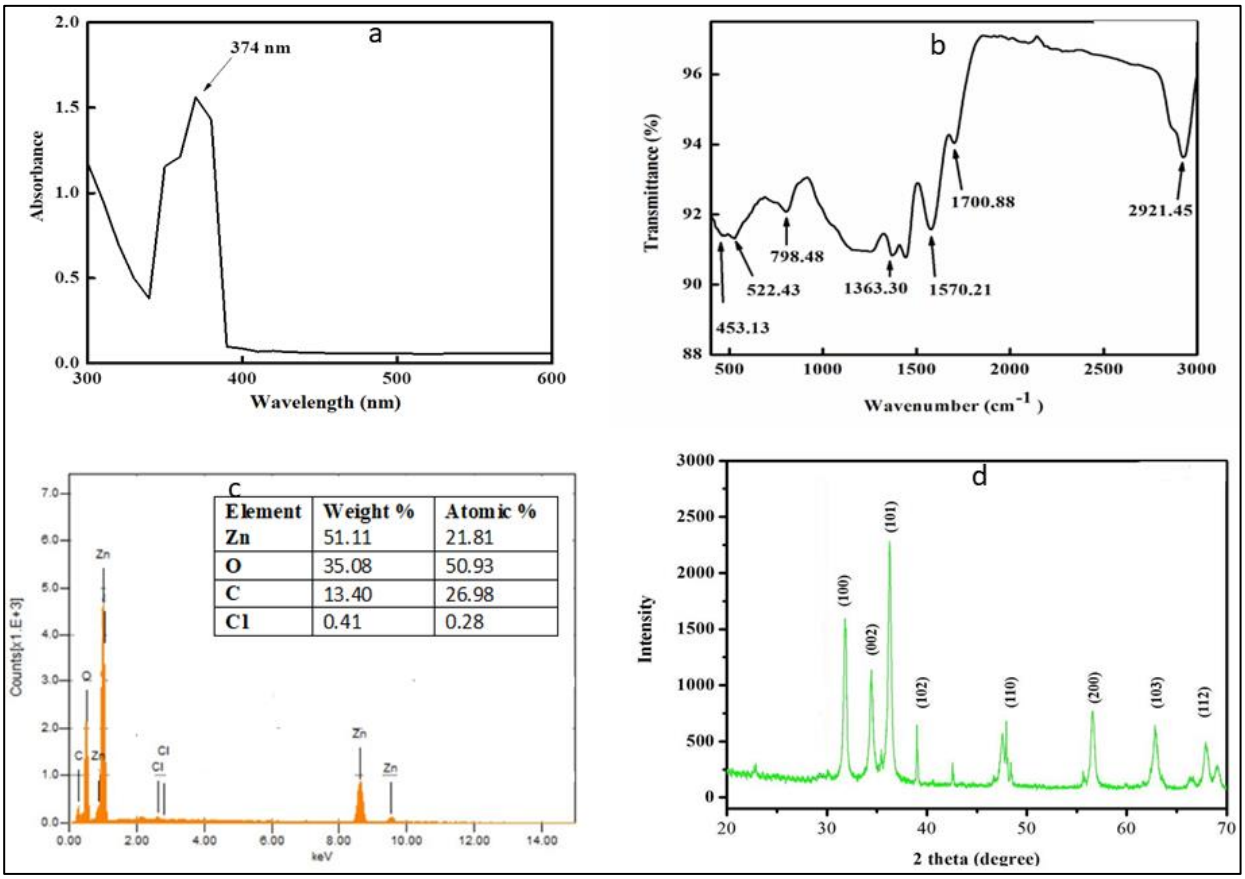

Figure 1. a) UV-Vis Absorption spectrum **b)** Representative FTIR analysis **c)** EDX spectrum **d)** XRD analysis of green synthesized zinc nanoparticles.

2.2. Energy-Dispersive X-Ray and X-Ray Diffraction Analysis

The EDX analysis showed the presence of various compounds on the surface of the synthesized nanoparticles as shown in Figure 1c. The quantitative and qualitative data from EDX regarding the sample's elemental makeup also confirm the formation of ZnNPs. The EDX spectrum of biosynthesized ZnNPs showed that Zn was present in substantial amounts (51.11 %) along with other elements including oxygen, carbon, chlorine that was also found in minor amounts and may have derived from the plant extract (Figure 1c). The minor peaks for Cl might be due to the precursor salt used in the synthesis of nanoparticles. Similarly, the XRD analysis for the structure and chemical composition of the synthesized nanoparticles are illustrated in Figure 1d. The results revealed that observed the sharps diffraction peaks could be used to easily index the hexagonal wurzite structure of ZnNPs. The peaks (100), (002), (101), (102), (110), (103), (200), and (112), corresponded to 2Θ of 31.821, 34.4651, 36.2886, 47.5941, 56.6508, 62.9114, 66.4064, 67.9868, 69.1113, 72.6063 and 76.9826, respectively. The sample exhibited identical patterns and lacked crystalline impurities thus indicating the phase purity of ZnNPs. The crystallite size of the ZnNPs was calculated from the most intense peak using Scherer's formulae and the crystallite size calculated for ZnNPs was found to be 66.20 nm (Figure 1d).

2.3. Scanning Electron Microscopic and Nano Measurer Particle Size Analysis

The SEM analysis was used to investigate the morphology and microstructure of the synthesised ZnNPs as shown in Figure 2a. The SEM micrograph of the biosynthesized ZnNPs demonstrated the presence of spherical-shaped nanoparticles. Likewise, the particle size was calculated from SEM

 doi:10.20944/preprints202404.0675.v2

image using nano-measurer software (Figure 2b). The results demonstrated that the calculated mean particle size was 9.61µm.

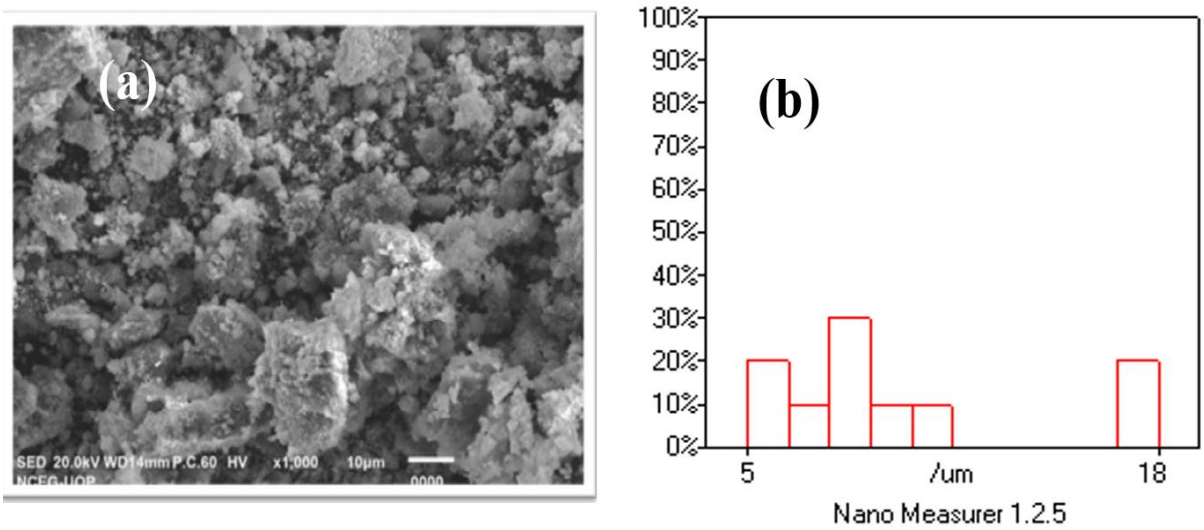

Figure 2. a) Scan Electron Microscopic image and **b)** nano-measurer particle size of synthesized zinc nanoparticles.

2.4. Antibacterial Activity

The findings of the antibacterial potential of the green synthesised ZnNPs assessed against the clinically isolated pathogenic bacteria such as *E. coli*, *S. aureus*, and *K. pneumoniae* are presented in Figure 3. It has been observed that ZnNPs inhibited the growth of *K. pneumonia* and *S. aureus* with zones of inhibition of 23 and 18 mm, respectively. Likewise in the case of *E. coli* the zone of inhibition was 16 mm. The obtained results are comparable with the tested standard antibiotic levofloxacin as shown in Figure 3. In addition, the investigated MIC and MBC values of the biosynthesized ZnNPs against *K. pneumoniae*, *S. aureus,* and *E.coli* were 34±0.21 and 72.71±0.47, 47±0.11 and 94.86±0.84 and 94±0.18 and 185.43±0.16µg/ml, respectively (Table 1).

Preprints.org (www.preprints.org) | NOT PEER-REVIEWED | Posted: 11 April 2024 doi:10.20944/preprints202404.0675.v2

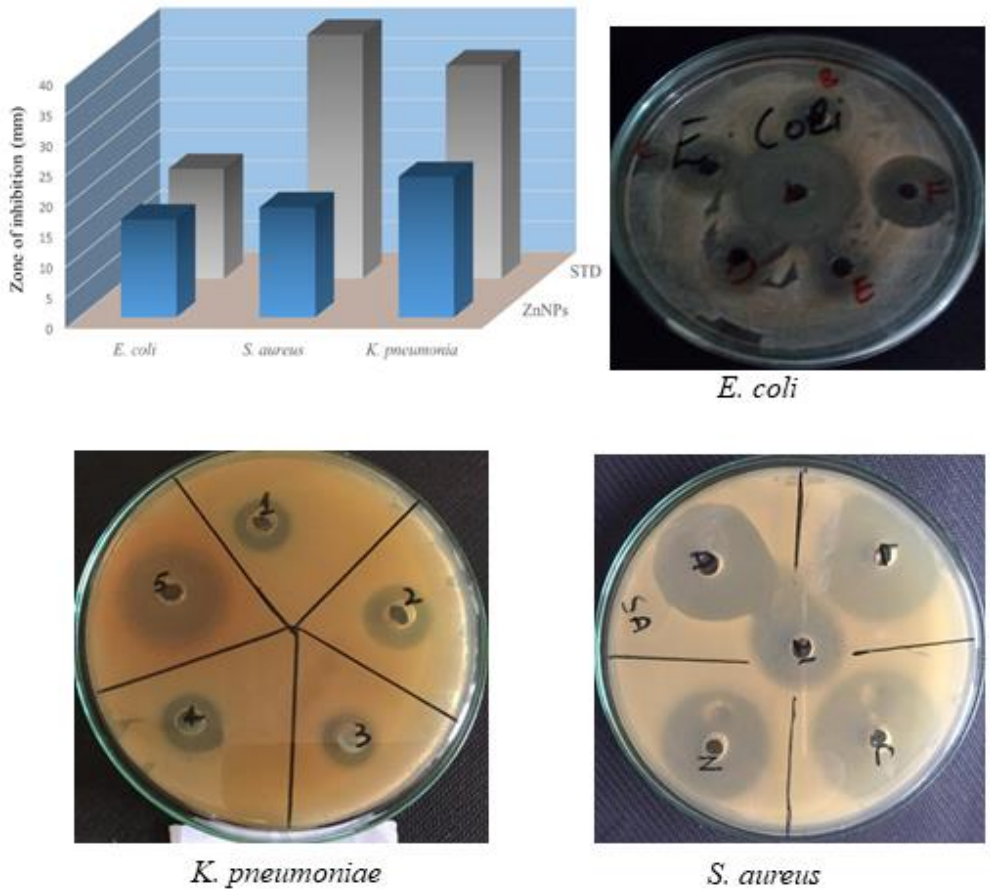

Figure 3. Antibacterial activity of synthesized zinc nanoparticles against *K. pneumonia*, *S. aureus* and *E.coli*

Table 1. Minimum inhibitory concentration (MIC) and minimum bactericidal concentration (MBC) values of biosynthesized ZnNPs pathogenic bacteria.

		MIC (µg/mL)			MBC (µg/mL)		
S.No	**Sample**	*E. coli*	*S. aureus*	*K. pneumoniae*	*E. coli*	*S. aureus*	*K. pneumoniae*
1	ZnNPS	94±0.18	47±0.11	34±0.21	185.43±0.16	94.86±0.84	72.71±0.47
2	Levofloxacin	11.72±0.82	0.35±0.11	50.17±0.41	23.43±1.03	7.82±0.45	97.75±0.9

δ Values are expressed as mean ± SD.

2.5. Membrane Damage Bioassay

The structural strength of the bacterial cell was determined by confirming the cell membrane injury by the biosynthesized ZnNPs. The results in the given Figure 4 depicts that the treatment of *E. coli*, *S. aureus,* and *K. pneumonia* with ZnNPs demonstrated a considerable increase in the concentration of intracellular contents. Moreover, the results clearly showed that the biosynthesized ZnNPs considerably damage the test bacterial membrane. It has been observed that the membrane damaging effect of ZnNPs was increased with an increase in the concentration and time of exposure as depicted by the elevated A_{260} values. In case of *K. pneumonia*, the membrane was seriously damaged with A_{260} value of 0.34 at 4 MIC and at 120 minutes of exposure. However, in case of *S. aureus* and *E. coli* the A_{260} values for extracellular substances released were 0.31 and 0.28 at 120 min of exposure at 4 MIC, respectively (Figure 4). It is thought that the basic mechanism behind damaging the bacterial cell might be the establishment of hydrogen bonds between the free NH group present in the biosynthesized ZnNPs and the peptidoglycan layer of the bacterial cell.

Preprints.org (www.preprints.org) | NOT PEER-REVIEWED | Posted: 11 April 2024 doi:10.20944/preprints202404.0675.v2

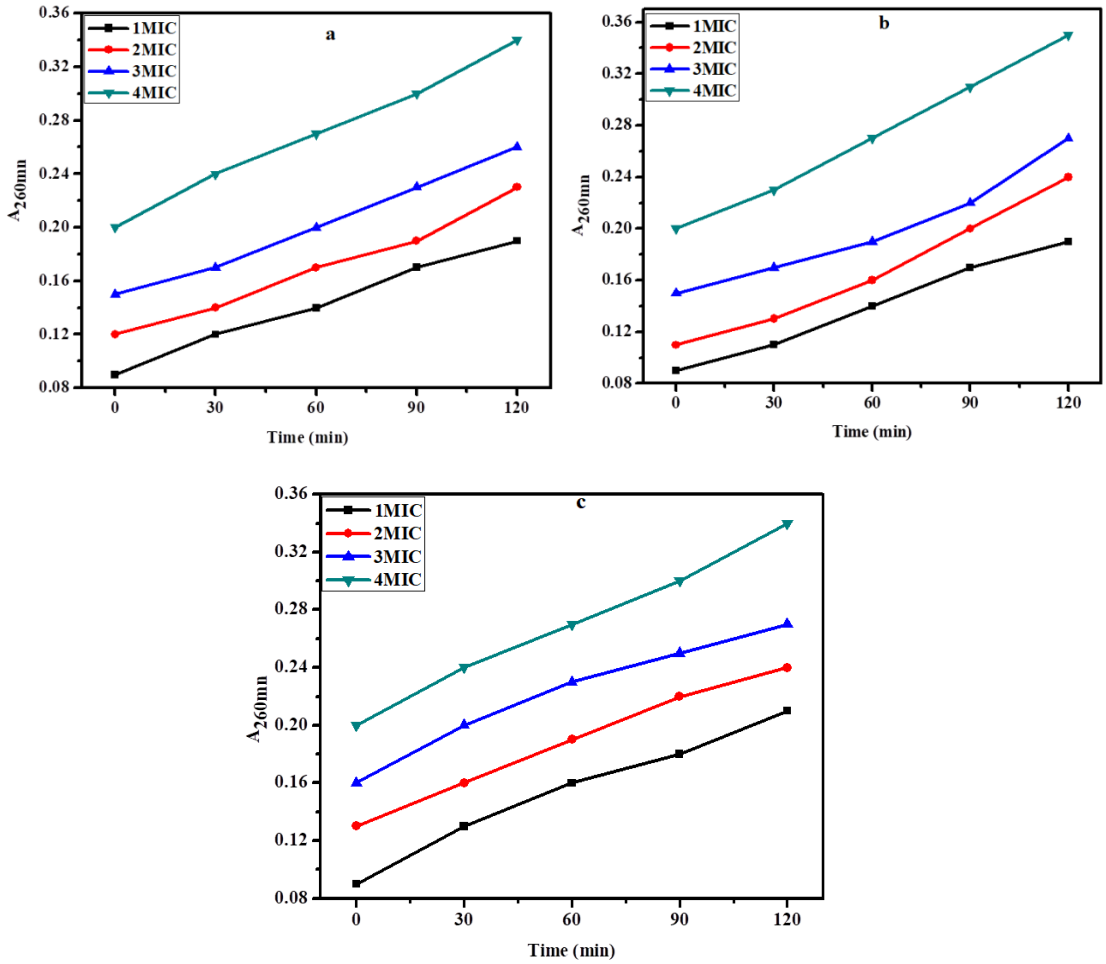

Figure 4. Effect of synthesized zinc nanoparticles on the release of intracellular materials from **(a)** *E. coli* **(b)** *S. aureus* and **(c)** *K. pneumoniae* cell suspensions at different times and concentrations.

2.6. Inner Membrane Permeability Bioassay

The destroying bacterial inner membrane is based on the enzyme β-galactosidase which is released when bacterial inner membranes get damaged. Lactose serves as β-galactosidase's real substrate and converts ONPG into o-nitrophenol which is a coloured product with the wavelength of 420 nm. In the current investigation, cells suspension was treated with different concentrations i.e., 1xMIC, 2xMIC, 3xMIC, and 4xMIC of ZnNPs, and the cleavage of ONPG was measured for 120 minutes and the results are plotted in Figures 5a, b, and c for *E. coli*, *S. aureus* and *K. pneumonia*, respectively. It has been observed that the hydrolysis rate of ONPG was increased with increase in the time of interaction ZnNPs with test bacterial strains. The overall findings revealed that for all test bacteria the utmost hydrolysis rate was recorded at the contact time of 120 minutes. Moreover, results showed that the green synthesized ZnNPs exhibited an effective inner membrane damaging action upon increasing the dose as well as time of interaction as showed by a greater A_{420} value, suggesting higher permeability of the bacterial membrane. The potential mechanisms for the bactericidal activity of these biosynthesized ZnNPs might be the membrane binding or its passive diffusion via the cell membrane, resulting in the membrane's permeability as shown in Figure 5 (a, b and c).

Preprints.org (www.preprints.org) | NOT PEER-REVIEWED | Posted: 11 April 2024 doi:10.20944/preprints202404.0675.v2

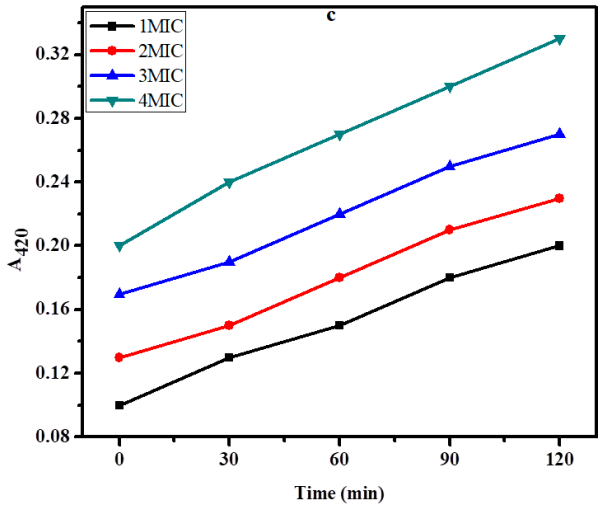

Figure 5. Release of cytoplasmic β-galactosidase from cell suspension of **(a)** *E. coli* **(b)** *S. aureus* **(c)** *K. pneumoniae* treated with synthesized zinc nanoparticles at different concentrations and time.

2.7. Hemolytic Activity

The results in Figure 6 depict the hemolytic effect of biosynthesized ZnNPs. The effect was studied at concentrations of 50, 100, 200, and 400 µg/mL of the test sample. The results demonstrated that the test sample caused 1, 1.3, 1.7, and 2.3 % lysis of red blood cells at 50, 100, 200, and 400 µg/mL, respectively. Conversely, Triton X-100 a standard haemolytic agent caused 87 % of hemolysis at 400 µg/mL. The comparison revealed that the biosynthesized ZnNPs showed no hemolysis at 400 µg/mL.

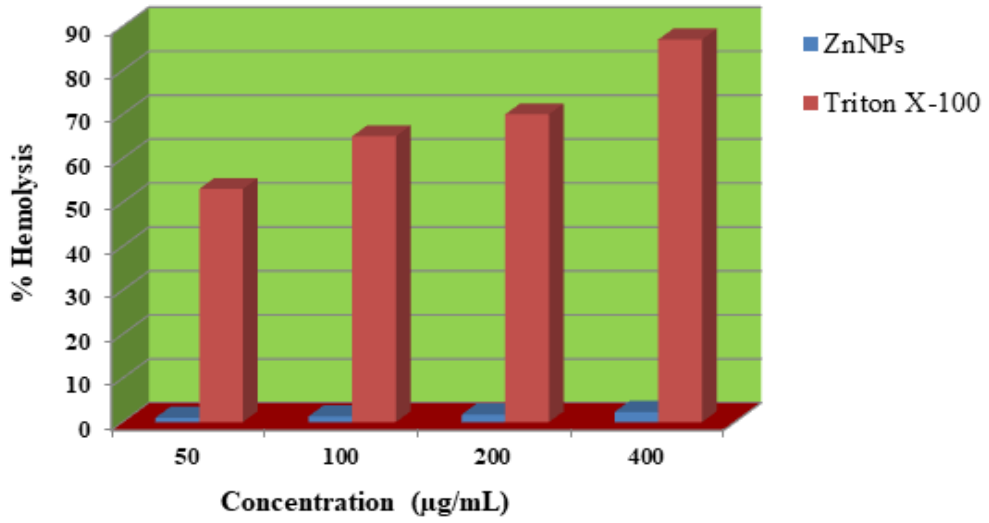

Figure 6. Hemlysis of red blood cells induced by synthesized zinc nanoparticles.

2.8. Photocatalytic Degradation of Synthetic Methyl Orange Dye

The biosynthesized ZnNPs was assessed to catalytically degrade the methyl orange dye and the results are presented in the Figure 7. It has been observed that the without nanoparticles no dye degradation was recorded hence confirm that solar irradiation had no effect on dye degradation. The results of the biosynthesized ZnNPs towards the degradation of methyl orange dye showed a broad absorption peak at 485 nm using UV-Visible spectrophotometer however a continuous decrease in the absorption intensity was recorded with time hence confirm that the tested ZnNPs pose higher ability to degrade the tested dye (Figure 7). It is clear that the photodegradation of methyl orange dye increased with increasing the irradiation contact time. The percent degradation showed that

 doi:10.20944/preprints202404.0675.v2

biosynthesized ZnNPs degrade around 19 % dye in 2 hours which increased to 37 % and 65 % by increasing the irradiation period to 4 hours and 6 hours, respectively as showed in Figure 7 (a and b).

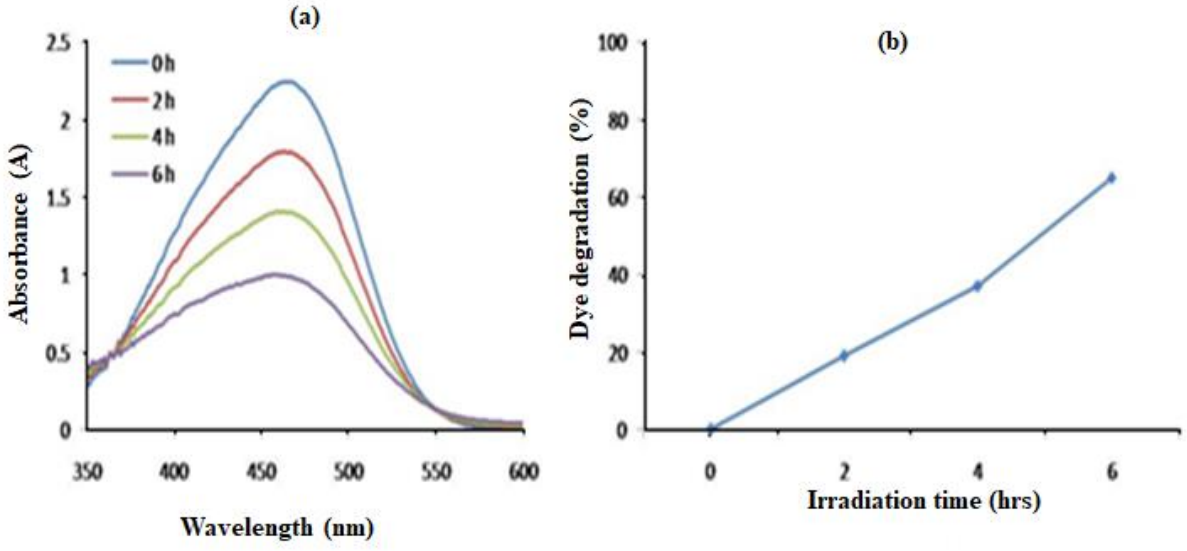

Figure 7. (a) Ultraviolet-visible spectrum of methyl orange dye by synthesized zinc nanoparticles and **(b)** Percent degradation of methyl orange dye by synthesized zinc nanoparticles.

3. Discussion

The current study is an effort for the biological fabrication of metal-based nanoparticles using plant parts to provide a novel, simple, and non-toxic protocol that can be utilized for antimicrobial and bioremediation applications. Plants and their parts are considered as a rich source of natural products and are attracting the attention of the scientific community for the wide range application including green synthesis of metal nanoparticles [21]. This investigation demonstrates the novel biological synthesis of ZnNPs from the bark extract of *R. arboreum* and were tested as antibacterial agent against clinically isolated pathogenic bacteria and environmental remediation for the photocatalytic degradation of methyl orange dye. *R. arboreum* possess wide range medicinal and antimicrobial applications due to the rich source of phytochemicals such as alkaloids, terpenoids, flavonoids, steroids, saponins, glycosides, tannins, anthraquinones, phlobatanins and reducing sugars [22]. Hence utilizing *R. arboretum*, these phytochemicals served as both reducing and capping agents for the formation of ZnNPs. The successful production of green synthesized ZnNPs were confirmed through UV absorption at 374 nm which confirmed the synthesis of ZnNPs. Likewise several other detailed characterizations were also performed for the synthesized ZnNPs. FTIR analysis was used to identify different types of functional groups in the *R. arboreum* bark extract that contributed to the biosynthesis of zinc nanoparticles. Likewise, SEM of biosynthesized ZnNPs revealed the presence of spherical, porous, and agglomerated nanoparticles particles. Moreover, the crystallite size of the biosynthesized nanoparticles was found to be 66.20 nm using XRD analysis. The characterizations affirm the successful synthesis of ZnNPs though the active constituents present in the *R. arboreum* bark extract that played an active role in inhibiting the degradation and deformation of formed ZnNPs. The MIC and MBC values of biosynthesized ZnNPs were found significant against *E. coli, S. aureus,* and *K. pneumonia*. The possible mechanism behind the bactericidal action of ZnNPs and the impact of biosynthesized ZnNPs on the membrane properties was assessed. Bacterial cell membrane is selective permeable barrier and is considered as one of the most important targets for antimicrobial agents[23]. Targeting and degrading this barrier by certain agents will lead to negative effects on the bacterial cell which may ultimately lead to the death of the bacterium cell[24]. It has been observed that biosynthesized ZnNPs effectively degrade the cell membrane by gradual leakage of compounds with absorbance at 260 nm after treatment with ZnNPs. Moreover, different types of methods could be utilized for determining the permeability of outer and inner membranes [25].

 doi:10.20944/preprints202404.0675.v2

Determination of the A_{260} value of intracellular compounds is one of the most important ones for assessing the integrity of the bacterial outer membrane. In the current investigation it has been observed that the green synthesized ZnNPs possess greater ability to damage the bacterial outer membrane as evidenced from the enhanced A_{260} value. It can be assumed that the green synthesized ZnNPs had disrupted the lipid-protein interactions in the bacterial membrane which in turn caused changes in the membrane permeability allowing the biosynthesized ZnNPs to enter into the cell. Nevertheless, for assessing the effect of ZnNPs on the permeability of the inner membrane ONPG method was used. This method is based on the fact that the bacteria lose control of the inner membrane permeability as the green synthesized ZnNPs penetrate into the bacterial cell [26]. The biosynthesized ZnNPs had increased the permeability of the bacterial inner membrane as evident from the increased production of o-nitrophenol a coloured product yielded after the hydrolysis of ONPG by β-galactosidase. On the basis of the obtained results the increase in the permeability of the inner and outer membranes of selected bacterial strains following treatment with ZnNPs suggested that these two processes may work in concert and that the end outcome of these two mechanisms was the death of the bacterial cells. Metal nanoparticles have a number of targets in the bacterial cell but primarily their antibacterial effect is exerted by interacting and damaging bacterial cell membranes [27].

Likewise, the catalytic activity of synthesized ZnNPs was also assessed based on the degradation of methyl orange dye under sunlight irradiation. The effective degradation of methyl orange dye under solar light illumination was studied at different time intervals. It has been observed that higher photodegradation (65%) of methyl orange dye was observed at the irradiation period of 6 hours. The high catalytic activity towards dye degradation attributed to synergetic properties of both Zn, *R. arboreum* and also nanostructural effect. Furthermore, the possible mechanism for the effective dye degradation by biosynthesized ZnNPs is the adsorption of dye over the surface of nanocomposite in the aqueous media[8] (Madhan et al., 2021). Following the adsorption, the dyes get excited during sun light irradiation and the excited dyes transfer e^- into the conduction band of Zn and thus cause the formation of e^- hole pairs (e^- /h^+) [28]. The pairs generate free radicals that are involved in the degradation of methyl orange and yield products such as CO_2 and H_2O [29] (Jiang et al., 2021). The findings of the current investigation confirmed that the biosynthesized ZnNPs a promising agent for the remediation of wastewater polluted with organic dye.

4. Materials and Methods

Bacterial strains such as *Escherichia coli* (ATCC 25922), *Staphylococcus aureus* (ATCC 25923) and *Klebsiella pneumoniae* (ATCC 43816) were collected from Pathology Department, Medical and Teaching Institute, Hayatabad Medical Complex Peshawar Pakistan as freeze dried culture and were stored at 4°C. Growth media such as nutrient agar and nutrient broth were obtained from Sigma Aldrich, USA. $ZnCl_2$ (99.9%) and other solvents used were purchased from Sigma Aldrich, USA and were of analytical grade.

4.1. Collection of Plant and Preparation of Plant Extract

R. arboreum plant was collected from Seran Valley Khyber Pakhtunkhwa, Pakistan and was authenticated by a botanist at Bacha Khan University, Charsadda-Pakistan. The bark of the collected plant was removed and washed with distilled water to remove the impurities and kept for drying. The dried bark (2.5 kg) was repeatedly extracted with methanol (3x5 L) at 25 °C. The methanolic extract was then filtered and further concentrated through a rotary evaporator until brownish crude methanolic extract. The obtained crude extract (~325 g) was then re-suspended in deionized water. The aqueous crude extract was then used for the synthesis of ZnNPs.

4.2. Biosynthesis and Characterization of Zinc Nanoparticles

0.1 M zinc chloride ($ZnCl_2$) was mixed with 25 mL of *R. arboreum* extract and was stirred for two hours. The progression of the reaction was monitored through UV spectrophotometer. The biosynthesized ZnNPs were then separated from the reaction solution through centrifugation at 6000

 doi:10.20944/preprints202404.0675.v2

rpm for 15 minutes. The precipitated ZnNPs were washed thrice with deionized water to remove the impurities and were dried subsequently. Finally, the purified ZnNPs were subjected to detailed characterization including UV-visible spectroscopy (UV-vis), Fourier Transform Infrared Spectroscopy (FTIR), Energy Dispersive X-ray spectroscopy (EDX), Scan Electron Microscopy (SEM), and X-Ray Diffraction (XRD) as per the standard protocols.

4.3. Antibacterial Screening

The antibacterial effects of biosynthesized ZnNPs were assessed using the well diffusion method. The bacterial inoculum comprised of *E. coli*, *S. aureus*, and *K. pneumoniae* was prepared under the instructions made by the National Committee for Clinical Laboratory Standards (NCCLS). Each bacterium was cultured in broth medium and incubated in a shaker incubator at 37 °C for 3 to 4 hours until a turbidity of 0.5 McFarland units was attained. With the use of a sterilized cotton swab, the culture of the test bacterium was distributed on the surface of agar plates and left to dry for 3 to 5 minutes. A sterile cork borer was used to gently bore the wells in the agar plate. The test sample and reference antibiotic were then added to the appropriate well and incubated for 24 hours at 37 °C. Using a slightly modified broth dilution method, the minimum inhibitory concentration (MIC) of ZnNPs was determined. The bacterial culture was injected into tubes with having sterilised broth medium. The test sample was added to the first tube so that the final concentration became 400 µg/mL and was serially diluted in a series of tubes having sterilized broth media to 12.5 µg/mL as the final concentration. The tubes were incubated for 24 hours at 37 °C. MIC was calculated as the lowest concentration of the test sample that inhibited the growth of bacteria. Minimum Bactericidal Concentration (MBC) of the test sample was obtained by streaking from the tubes used for MIC on agar plates with subsequent incubation for a period of 24 hrs at 37 °C. The MBC was determined to be the lowest concentration of the test sample at which the bacterium did not show growth on an agar plate. Results of the test and standard antibiotic levofloxacin were measured in mm.

4.4. Membrane Damage Assay

The effect in term of cell membrane disturbance was analyzed by measuring the A_{260} value of the intracellular substances that were released upon the interactions of ZnNPs with the bacterial cells. The culture was refreshed for 24 hours by transferring inoculum to broth medium from the agar plate followed by incubation at 37 °C. Centrifugation of the refreshed culture was performed at 10,000 rpm for 10 minutes. The bacterial pellet collected was thoroughly washed with Phosphate-buffered saline (PBS) and suspended again in 0.01 mol L^{-1} PBS solution and the optical density was set to 0.7 at 420 nm. Finally, 1.5 mL of different concentrations of test complexes was treated with 1.5 mL of test bacteria and the quantity of released intracellular substances was measured spectrophotometrically at 260 nm.

4.5. Inner Membrane Permeabilization Bioassay

In this assay, the released β-galactosidase enzyme was determined using the procedure reported by [30]. Test inoculum was prepared in broth medium having 2 % of lactose. Then the bacterial cells were harvested by centrifugation and re-suspended in 0.01 mol L^{-1} PBS solution and the absorbance of the cell suspension was adjusted to 1.2 at 420 nm. Furthermore, test samples (1.6 mL) at different concentrations were added to the culture (1.6 mL) followed by the addition of 150 µl of 30 Mm O-nitrophenyl-beta-D-galactopyranoside (ONPG) and thorough mixing *o*-nitrophenol produced at different time intervals was measured at 420 nm.

4.6. Hemolytic Assay

To avoid blood coagulation, blood samples were taken from human donors in K_2-EDTA tubes. Centrifugation was done at 14000 rpm for 5 minutes and the plasma was gently aspirated and the cell pellet was washed 3 times with PBS (pH 7.4). Diluted RBCs were mixed with varying concentrations of the test sample (1:1 ratio). Triton X-100 (20 %) and PBS were used as positive and negative controls, respectively [31]. All the tubes were shaken for 1 hour at 37 °C before being centrifuged for 5 minutes

 doi:10.20944/preprints202404.0675.v2

at 14000 rpm to pellet the cells. The upper portion was collected in a clean test tube and the absorbance was checked at 540 nm. The following equation 1 was used for the determination of percent hemolysis.

$$\%\ Hemolysis = \frac{At-An}{Ap-An} \times 100 \qquad \text{Equation 1}$$

Where

At is the absorbance of test sample.

An is the absorbance of the negative control (PBS)

Ap is the absorbance of the positive control (Triton-X-100)

4.7. *Photocatalytic Degradation of Synthetic Methyl Orange Dye*

The synthesized ZnNPs were assessed for the degradation of synthetic methyl orange dye using sunlight as source of energy. Initially, the dye was kept in the sunlight without nanoparticles but no degradation of dye was noticed showing that solar irradiation had no effect on dye degradation. A beaker containing 10 mL methyl orange (25 ppm) and 0.1 mg of nanoparticles was kept to sunlight while being stirred continuously. The photodegradation reactions were conducted at Bacha Khan University, Pakistan in direct sunshine at coordinates of 39°9°N and 71°44°E. The reaction was first run in complete darkness for 30 minutes to confirm adsorption and desorption equilibrium. Correspondingly in direct sunlight, the reactions were performed for 30 minutes and aliquots of the reaction were taken at predetermined intervals while being exposed to solar light irradiations. Al the end of each experimental run the solution was centrifuged at 14,000 rpm and was subjected to UV-vis spectrophotometric analysis. For the determination of percent degradation following equation II and III was used.

$$\text{Degradation rate (\%)} = \left(\frac{C_0-C}{C_0}\right) \times 100 \qquad \text{Equation II}$$

$$\text{Degradation rate (\%)} = \left(\frac{A_0-A}{A_0}\right) \times 100 \qquad \text{Equation III}$$

where Co is the initial dye concentration, C is the dye concentration after UV irradiation, Ao shows initial absorbance, and A is the dye absorbance after UV irradiation.

4.8. Statistical Analysis

All the experimental trails were performed in triplicates and data were expressed as mean ±SD. Moreover, one-way analysis of variance (ANOVA) with Tukey's posthoc test was performed to find significant differences (p<0.05).

Conclusions

The current study employed a novel green synthesis of ZnNPs using the bark extract of *R. arboreum*. The biosynthesized ZnNPs were confirmed by the detailed characterizations including UV-Vis, FTIR, EDX, XRD, and SEM. The biosynthesized ZnNPs were proved to be a good antibacterial agent inhibiting the growth of *E. coli*, *S. aureus*, and *K. pneumonia*. Moreover, the MIC and MBC values of the biosynthesized ZnNPs against *K. pneumonia*, *S. aureus*, and *E.coli* were 34±0.21 and 11.71±0.47, 47±0.11 and 23.86±0.84 and 94±0.18 and 40.43±0.16 µg/ml, respectively. The biosynthesized ZnNPs also pose serious damaged the outer and inner membrane in the first phase of exposure causing the death of bacterial cells. However, the utmost membrane damaged was observed at 120 minutes of exposure. Interestingly, biosynthesized ZnNPs showed no hemolysis in comparison to Triton X-100 a standard haemolytic agent. In addition to the antibacterial activities, the biosynthesized ZnNPs also exhibited significant catalytic activity towards the degradation of methyl orange dye. The results demonstrated that the rate of photodegradation of methyl orange was increased exposure time and reached to 65 % by reaching the irradiation period to 6 hours. This study therefore concluded that *R. arboreum* based ZnNPs are capable of effectively controlling pathogenic bacteria and can be applied for water purification through photocatalytic degradation of dye. However, the key constrain of using nanoparticles against microbial activities and dyes removal is the complete separation form treated media. In this regard, several attempts have been made for the separation for the purpose to regenerate and it recycles back for reuse. However, the dual approach of removal and regeneration

 doi:10.20944/preprints202404.0675.v2

is still at exploratory stage that also requires extensive research for successful exploration. Furthermore, keeping in view the real environmental systems with high microbial and pollutants heterogeneity and complexity, there is dire need of exploration of the potential of the biosynthesized ZnNPs in the real environment.

Declaration of competing interest: The authors of this article have no conflict of interest.

Acknowledgments: The authors wish to thank the Researchers Supporting Project number (RSP2024R346) at King Saud University Riyadh Saudi Arabia for financial support.

References

1. Ahmad, A.; Khan, M.; Sufyan Javed, M.; Hassan, A.M.; Choi, D.; Khawar, M.R.; Waqas, M.; Ayub, A.; Alothman, A.A.; Almuhous, N.A. Eco-Benign Synthesis of α-Fe2O3 Mediated Trachyspermum Ammi: A New Insight to Photocatalytic and Bio-Medical Applications. *J. Photochem. Photobiol. A Chem.* **2024**, *449*, 115423, doi:10.1016/j.jphotochem.2023.115423.
2. Darra, R.; Hammad, M. Bin; Alshamsi, F.; Alhammadi, S.; Al-Ali, W.; Aidan, A.; Tawalbeh, M.; Halalsheh, N.; Al-Othman, A. Wastewater Treatment Processes and Microbial Community. In *Metagenomics to Bioremediation: Applications, Cutting Edge Tools, and Future Outlook*; 2022; pp. 329–355 ISBN 9780323961134.
3. Salam, M.A.; Al-Amin, M.Y.; Salam, M.T.; Pawar, J.S.; Akhter, N.; Rabaan, A.A.; Alqumber, M.A.A. Antimicrobial Resistance: A Growing Serious Threat for Global Public Health. *Healthc.* 2023, *11*.
4. Sudarshan, S.; Harikrishnan, S.; RathiBhuvaneswari, G.; Alamelu, V.; Aanand, S.; Rajasekar, A.; Govarthanan, M. Impact of Textile Dyes on Human Health and Bioremediation of Textile Industry Effluent Using Microorganisms: Current Status and Future Prospects. *J. Appl. Microbiol.* 2023, *134*.
5. Islam, T.; Repon, M.R.; Islam, T.; Sarwar, Z.; Rahman, M.M. *Impact of Textile Dyes on Health and Ecosystem: A Review of Structure, Causes, and Potential Solutions*; Springer Berlin Heidelberg, 2023; Vol. 30; ISBN 0123456789.
6. Jorge, A.M.S.; Athira, K.K.; Alves, M.B.; Gardas, R.L.; Pereira, J.F.B. Textile Dyes Effluents: A Current Scenario and the Use of Aqueous Biphasic Systems for the Recovery of Dyes. *J. Water Process Eng.* **2023**, *55*, 104125, doi:10.1016/j.jwpe.2023.104125.
7. Hasan, S.; Rauf, A. Role of Nanomaterials for Removal of Biomaterials and Microbes from Wastewater. In *Nanotechnology Horizons in Food Process Engineering*; 2023; pp. 303–342.
8. Madhan, G.; Begam, A.A.; Varsha, L.V.; Ranjithkumar, R.; Bharathi, D. Facile Synthesis and Characterization of Chitosan/zinc Oxide Nanocomposite for Enhanced Antibacterial and Photocatalytic Activity. *Int. J. Biol. Macromol.* **2021**, *190*, 259–269, doi:10.1016/j.ijbiomac.2021.08.100.
9. Motakef-Kazemi, N.; Yaqoubi, M. Green Synthesis and Characterization of Bismuth Oxide Nanoparticle Using Mentha Pulegium Extract. *Iran. J. Pharm. Res.* **2020**, *19*, 70–79, doi:10.22037/ijpr.2019.15578.13190.
10. Fritea, L.; Banica, F.; Costea, T.O.; Moldovan, L.; Dobjanschi, L.; Muresan, M.; Cavalu, S. Metal Nanoparticles and Carbon-Based Nanomaterials for Improved Performances of Electrochemical (Bio)sensors with Biomedical Applications. *Materials (Basel).* **2021**, *14*, doi:10.3390/ma14216319.
11. Mba, I.E.; Nweze, E.I. Nanoparticles as Therapeutic Options for Treating Multidrug-Resistant Bacteria: Research Progress, Challenges, and Prospects. *World J. Microbiol. Biotechnol.* 2021, *37*.
12. Thambirajoo, M.; Maarof, M.; Lokanathan, Y.; Katas, H.; Ghazalli, N.F.; Tabata, Y.; Fauzi, M.B. Potential of Nanoparticles Integrated with Antibacterial Properties in Preventing Biofilm and Antibiotic Resistance. *Antibiotics* 2021, *10*.
13. Islam, M.; Kumar, S.; Saxena, N.; Nafees, A. Photocatalytic Degradation of Dyes Present in Industrial Effluents: A Review. *ChemistrySelect* 2023, *8*.
14. Hachem, K.; Ansari, M.J.; Saleh, R.O.; Kzar, H.H.; Al-Gazally, M.E.; Altimari, U.S.; Hussein, S.A.; Mohammed, H.T.; Hammid, A.T.; Kianfar, E. Methods of Chemical Synthesis in the Synthesis of Nanomaterial and Nanoparticles by the Chemical Deposition Method: A Review. *Bionanoscience* 2022, *12*, 1032–1057.
15. Qamar, S.U.R.; Ahmad, J.N. Nanoparticles: Mechanism of Biosynthesis Using Plant Extracts, Bacteria, Fungi, and Their Applications. *J. Mol. Liq.* **2021**, *334*, doi:10.1016/j.molliq.2021.116040.
16. Ezealigo, U.S.; Ezealigo, B.N.; Aisida, S.O.; Ezema, F.I. Iron Oxide Nanoparticles in Biological Systems: Antibacterial and Toxicology Perspective. *JCIS Open* 2021, *4*.
17. Shafey, A.M. El Green Synthesis of Metal and Metal Oxide Nanoparticles from Plant Leaf Extracts and Their Applications: A Review. *Green Process. Synth.* 2020, *9*, 304–339.
18. Sidhu, A.K.; Verma, N.; Kaushal, P. Role of Biogenic Capping Agents in the Synthesis of Metallic Nanoparticles and Evaluation of Their Therapeutic Potential. *Front. Nanotechnol.* 2022, *3*.

19. Mehta, J.; Rolta, R.; Salaria, D.; Ahmed, A.; Chandel, S.R.; Regassa, H.; Alqahtani, N.; Ameen, F.; Amarowicz, R.; Gudeta, K. In Vitro and in Silico Properties of Rhododendron Arboreum against Pathogenic Bacterial Isolates. *South African J. Bot.* **2023**, *161*, 711–719, doi:10.1016/j.sajb.2023.08.014.
20. Sharma, S.; Chaudhary, S.; Harchanda, A. Rhododendron Arboreum : A Critical Review on Phytochemicals, Health Benefits and Applications in the Food Processing Industries . *Curr. Nutr. Food Sci.* **2021**, *18*, 287–304, doi:10.2174/1573401317666210921104622.
21. Saleem, S.; Ahmed, B.; Khan, M.S.; Al-Shaeri, M.; Musarrat, J. Inhibition of Growth and Biofilm Formation of Clinical Bacterial Isolates by NiO Nanoparticles Synthesized from Eucalyptus Globulus Plants. *Microb. Pathog.* **2017**, *111*, 375–387, doi:10.1016/j.micpath.2017.09.019.
22. Nisar, M.; Ali, S.; Qaisar, M. Preliminary Phytochemical Screening of Flowers , Leaves , Bark , Stem and Roots of Rhododendron Arboreum. *Middle-East J. Sci. Res.* **2011**, *10*, 472–476.
23. Varela, M.F.; Stephen, J.; Lekshmi, M.; Ojha, M.; Wenzel, N.; Sanford, L.M.; Hernandez, A.J.; Parvathi, A.; Kumar, S.H. Bacterial Resistance to Antimicrobial Agents. *Antibiotics* 2021, *10*.
24. Panchal, P.; Paul, D.R.; Sharma, A.; Choudhary, P.; Meena, P.; Nehra, S.P. Biogenic Mediated Ag/ZnO Nanocomposites for Photocatalytic and Antibacterial Activities towards Disinfection of Water. *J. Colloid Interface Sci.* **2020**, *563*, 370–380, doi:10.1016/j.jcis.2019.12.079.
25. Frallicciardi, J.; Melcr, J.; Siginou, P.; Marrink, S.J.; Poolman, B. Membrane Thickness, Lipid Phase and Sterol Type Are Determining Factors in the Permeability of Membranes to Small Solutes. *Nat. Commun.* **2022**, *13*, doi:10.1038/s41467-022-29272-x.
26. Bouyahya, A.; Abrini, J.; Dakka, N.; Bakri, Y. Essential Oils of Origanum Compactum Increase Membrane Permeability, Disturb Cell Membrane Integrity, and Suppress Quorum-Sensing Phenotype in Bacteria. *J. Pharm. Anal.* **2019**, *9*, 301–311, doi:10.1016/j.jpha.2019.03.001.
27. Ahmed, B.; Hashmi, A.; Khan, M.S.; Musarrat, J. ROS Mediated Destruction of Cell Membrane, Growth and Biofilms of Human Bacterial Pathogens by Stable Metallic AgNPs Functionalized from Bell Pepper Extract and Quercetin. *Adv. Powder Technol.* **2018**, *29*, 1601–1616, doi:10.1016/j.apt.2018.03.025.
28. Anh Tran, V.; Khoa Phung, T.; Thuan Le, V.; Ky Vo, T.; Tai Nguyen, T.; Anh Nga Nguyen, T.; Quoc Viet, D.; Quang Hieu, V.; Thi Vo, T.T. Solar-Light-Driven Photocatalytic Degradation of Methyl Orange Dye over Co3O4-ZnO Nanoparticles. *Mater. Lett.* **2021**, *284*, doi:10.1016/j.matlet.2020.128902.
29. Jiang, R.; Zhu, H.Y.; Fu, Y.Q.; Jiang, S.T.; Zong, E.M.; Zhu, J.Q.; Zhu, Y.Y.; Chen, L.F. Colloidal CdS Sensitized Nano-ZnO/chitosan Hydrogel with Fast and Efficient Photocatalytic Removal of Congo Red under Solar Light Irradiation. *Int. J. Biol. Macromol.* **2021**, *174*, 52–60, doi:10.1016/j.ijbiomac.2021.01.077.
30. Liu, H.; Du, Y.; Wang, X.; Sun, L. Chitosan Kills Bacteria through Cell Membrane Damage. *Int. J. Food Microbiol.* **2004**, *95*, 147–155, doi:10.1016/j.ijfoodmicro.2004.01.022.
31. Lee, J.K.; Park, S.C.; Hahm, K.S.; Park, Y. A Helix-PXXP-Helix Peptide with Antibacterial Activity without Cytotoxicity against MDRPA-Infected Mice. *Biomaterials* **2014**, *35*, 1025–1039, doi:10.1016/j.biomaterials.2013.10.035.